UDC 546.06, 538.91, 539.8
https://doi.org/10.17073/0021-3438-2025-1-27-40

Research article
Научная статья

Production of cast master alloys with high chromium content using centrifugal SHS metallurgy

A.N. Kubanova[1,2], **D.M. Ikornikov**[1], **V.N. Sanin**[1], **D.A. Martynov**[3]

[1] **Merzhanov Institute of Structural Macrokinetics and Materials Science of the Russian Academy of Sciences**
8 Academician Osipyan Str., Chernogolovka, Moscow Region 142432, Russia

[2] **Tula State Pedagogical University n.a. L.N. Tolstoy**
125 Lenin Prosp., Tula 300026, Russia

[3] **LLC "Research, Design and Technology Center"**
4 Bld, 102 Lenin Prosp., Tula 300025, Russia

✉ Anastasiya N. Kubanova (kubanovaan@tspu.ru)

Abstract: Cast master alloys of the Mo–Cr, W–Cr, and Cr–Al systems with high chromium content were produced using the methods of centrifugal SHS metallurgy. A thermodynamic analysis was performed to evaluate the combustion temperature and the equilibrium composition of the reaction products depending on the ratios of the initial components in the mixture. Based on this analysis, optimal compositions were identified for further experimental studies. The effectiveness of functional additives, namely calcium fluoride CaF_2 (fluorspar) and sodium hexafluoroaluminate $Na_3[AlF_6]$ (cryolite), was experimentally confirmed. These additives were shown to lower the melting point of the slag phase (reducing its viscosity), which facilitated phase separation during the production of cast master alloys from refractory metals using centrifugal SHS metallurgy. The experiments demonstrated the need to introduce excess amounts of MoO_3 and WO_3 during the production of Mo–Cr and W–Cr master alloys, respectively, due to incomplete reduction of molybdenum and tungsten from their oxides. Microstructural analysis of the obtained master alloys revealed a dendritic structure, which is typical for cast materials. EDS microanalysis showed that the chemical compositions of all synthesized alloys closely matched their calculated and target compositions. Composition analysis at different locations within the ingots revealed no significant variations in composition. *X*-ray phase analysis confirmed the presence of solid solution phases formed from the target elements. The results of inductively coupled plasma mass spectrometry (ICP-MS) confirmed that the chemical compositions of the synthesized Cr–W, Cr–Mo, and Cr–Al alloys fully comply with the permissible concentrations of both target elements and impurities.

Keywords: master alloy, chromium, molybdenum, tungsten, aluminum, self-propagating high-temperature synthesis, centrifugal SHS metallurgy.

For citation: Kubanova A.N., Ikornikov D.M., Sanin V.N., Martynov D.A. Production of cast master alloys with high chromium content using centrifugal SHS metallurgy. *Izvestiya. Non-Ferrous Metallurgy*. 2025;31(1):27–40. https://doi.org/10.17073/0021-3438-2025-1-27-40

Получение литых лигатур с высоким содержанием Cr методами центробежной СВС-металлургии

А.Н. Кубанова[1,2], **Д.М. Икорников**[1], **В.Н. Санин**[1], **Д.А. Мартынов**[3]

[1] **Институт структурной макрокинетики и проблем материаловедения им. А.Г. Мержанова РАН**
Россия, 142432, Московская обл., г. Черноголовка, ул. Академика Осипьяна, 8

[2] **Тульский государственный педагогический университет им. Л.Н. Толстого**
Россия, 300026, г. Тула, пр-т Ленина, 125

[3] **ООО «Центр исследований, дизайна и технологий»**
Россия, 300025, г. Тула, пр-т Ленина, 102, к. 4

✉ Анастасия Николаевна Кубанова (kubanovaan@tspu.ru)

Аннотация: Методами центробежной СВС-металлургии получены литые лигатуры Mo–Cr, W–Cr и Cr–Al с высоким содержанием Cr. Выполнен термодинамический анализ температуры горения и состава равновесных продуктов в зависимости от соотношения исходных компонентов смеси. На основе анализа определены оптимальные составы для проведения экспериментальных исследований. Экспериментально установлена эффективность применения функциональных добавок CaF_2 (плавиковый шпат) и гексафтороалюмината натрия $Na_3[AlF_6]$ (криолит) с целью снижения температуры плавления шлаковой фазы (уменьшения ее вязкости) и облегчения процесса фазоразделения при производстве литых лигатур из тугоплавких металлов методом центробежной СВС-металлургии. Анализ экспериментов показал необходимость ввода избыточного содержания MoO_3 и WO_3 при производстве лигатур Mo–Cr и W–Cr соответственно ввиду неполного восстановления Mo и W из их оксидов. Анализ микроструктуры полученных лигатур свидетельствует о наличии дендритной структуры, что типично для литого состояния сплавов. По результатам микроанализов (EDS), все полученные лигатуры близки к своим расчетным и целевым значениям химических составов. Микроанализ состава разных участков слитков не выявил заметных различий по составу сплава. Проведенные рентгенофазовые анализы синтезируемых лигатур показали наличие пиков твердых растворов, сформированных на основе соответствующих целевых элементов. Анализ данных химического состава, полученного с помощью метода масс-спектроскопии с индуктивно-связанной плазмой, для синтезированных сплавов систем Cr–W, Cr–Mo и Cr–Al выявил их полное соответствие значениям по допустимым концентрациям как целевых элементов, так и примесных компонентов.

Ключевые слова: лигатура, хром, молибден, вольфрам, алюминий, самораспространяющийся высокотемпературный синтез, центробежная СВС-металлургия.

Для цитирования: Кубанова А.Н., Икорников Д.М., Санин В.Н., Мартынов Д.А. Получение литых лигатур с высоким содержанием Cr методами центробежной СВС-металлургии. *Известия вузов. Цветная металлургия*. 2025;31(1):27–40.
https://doi.org/10.17073/0021-3438-2025-1-27-40

Introduction

Alloying technologies for modern industrial alloys have become widely used across various industries. The optimal selection of alloying component compositions and alloying methods enables the resolution of complex challenges in the design and manufacturing of diverse products, achieving the desired combination of performance characteristics [1; 2]. The introduction of master alloys with a specified composition allows for precise control of alloying element concentrations and ensures the efficient introduction of easily oxidizable or volatile components into the melt at high temperatures, as these components are supplied in a stable cast (pre-alloyed) form.

Currently, the primary industrial method for producing most master alloys involves the direct melting of metals using electrometallurgical techniques. This method is associated with high energy and material costs, largely due to the need for high-purity starting materials. Moreover, when using components with significantly different melting points, losses of volatile elements increase, which negatively affects both the quality of the master alloy and the final production cost of industrial alloys.

Cast chromium-based master alloys of various compositions (Cr—Al, Cr—Cu, Cr—Fe, Cr—Ti, Cr—V—Al, etc.) have already become well-established in the metallurgical industry as alloying additives in the production of high-alloy steels, heat-resistant nickel alloys, aluminum alloys, and others [3; 4]. Since chromium has a melting point of approximately 1900 °C, it cannot be melted in a vacuum due to sublimation (direct transition from solid to gas) [3]. Therefore, the production of high-chromium master alloys requires melting the starting metals in an inert gas atmosphere at pressures exceeding 760 mmHg, which significantly complicates the technological process.

As a result, the production of chromium-containing master alloys, where components have significantly different melting points, presents several challenges when using conventional metallurgical methods [5]. The large difference in melting points between aluminum and chromium makes the production of Cr—Al master alloys particularly costly due to the significant evaporation of aluminum during melting, or it necessitates the use of multi-stage powder metallurgy techniques requiring extremely pure starting materials [5]. The high melting points of tungsten, molybdenum, and chromium make it impossible to produce these alloys using traditional melting of charge materials. Due to this characteristic, the conventional production of Mo—Cr and W—Cr alloys relies on two main technological approaches:

— expensive vacuum arc and electron beam remelting processes, which result in significant material losses due to evaporation at high temperatures;

— powder metallurgy methods, which involve multi-stage pressing of high-purity metal powders, usually followed by sintering in inert or reactive gas atmospheres (nitrogen, argon, or hydrogen).

Therefore, there is a clear need to improve the energy efficiency of master alloy production for systems with significantly different melting points, while reducing production costs without compromising material properties and quality.

One of the relatively recent methods for producing cast and powder materials based on metals and their compounds is Self-Propagating High-Temperature Synthesis (SHS) [6; 7], which has already been applied in the production of master alloys used to develop new high-strength structural alloys, including those intended for service in Arctic conditions [8—10]. One important technological branch of SHS processes is centrifugal SHS metallurgy [11—13], which combines SHS with metallothermy [14]. The key feature of SHS metallurgy lies in conducting highly exothermic reduction reactions while applying additional physical forces (centrifugal forces), which enables the production of high-quality cast combustion products. This approach also serves as an additional tool for controlling the formation of composition and structure in the resulting cast SHS materials [11; 15; 16—18].

The objective of this study was to develop the chemical and technological foundations for the synthesis of high-chromium alloys (Cr—Mo, Cr—W, Cr—Al) by means of centrifugal SHS metallurgy.

Research materials and methods

The process used to produce the alloys under investigation is based on an exothermic reaction between the oxides of the target metals (Cr, W, and Mo) and aluminum (acting as a metallic reducing agent), which proceeds in a self-propagating combustion (SHS) mode. This reaction is accompanied by the melting (casting) of the final products, followed by their phase separation under the influence of centrifugal forces generated in the centrifugal SHS setup.

The overall chemical equations describing the synthesis of the studied alloys can be represented as follows:

$$Cr_2O_3 + MoO_3 + \alpha Al + FA \rightarrow \rightarrow Cr{—}Mo\ (Al) + Al_2O_3, \quad (1)$$

$$Cr_2O_3 + WO_3 + \alpha Al + FA \rightarrow \rightarrow Cr{—}W\ (Al) + Al_2O_3, \quad (2)$$

$$[Cr_2O_3\ /CrO_3] + \alpha Al + FA \rightarrow \rightarrow Cr{—}Al + Al_2O_3, \quad (3)$$

where FA denotes a functional additive based on fluorite CaF_2 (fluorspar) and cryolite $Na_3[AlF_6]$ (sodium hexafluoroaluminate).

Table 1 presents the grades and selected characteristics of the raw materials reagents used in the study. The functional additives were introduced into the reaction mixture as a combination of these two compounds (cryolite and fluorspar) to facilitate phase separation of the reaction products.

The target compositions of the Mo—Cr, W—Cr, and Cr—Al master alloys were selected based on actual chemical compositions used at leading metallurgical enterprises in Russia (Table 2). The permissible concentration ranges for the elements in this group of alloys were provided by a potential end user of the research results — Electrostal Metallurgical Plant JSC (Electrostal, Moscow Region).

Table 1. **Selected characteristics of raw materials and functional additives**

Таблица 1. Некоторые характеристики исходных веществ и ФД

Material	Grade	Standard (GOST/TU)	Particle size, μm	Purity, %
		Main components for synthesis		
Cr_2O_3	Ch	TU 6-09-4272-84	<20	99.00
WO_3	ChDA	TU 48-4205-122-2019	<20	99.90
MoO_3	ChDA	TU 6-09-4471-77	<50	99.00
Al	PA-4	GOST 6058-73	<140	98.00
		Functional additives (FA)		
CaO	Pure	GOST 8677-76	<150	96.0
$Na_3[AlF_6]$	KP	GOST 10561-80	<150	97.0
CaF_2	FF-97	GOST 29219-91	<100	97.2

Table 2. **Permissible element concentrations in the chemical compositions of the studied alloys**

Таблица 2. Допустимые концентрации элементов по химическому составу для исследуемых сплавов

Element, wt. %	Alloy system		
	Cr–W (Al)	Cr–Mo (Al)	Cr–Al
Cr	Balance	Balance	Balance
Mo	1.0	50–65	–
W	40–60	–	–
Al	–	–	10–25
Impurities, not more than			
Al	5.0	5.0	–
C	0.05	0.05	0.04
Si	0.3	0.3	0.5
S	0.01	0.01	0.01
P	0.01	0.01	0.01
Fe	1.0	1.0	0.7
Cu	0.05	0.05	0.2
Co	0.1	0.1	–
O	0.04	0.05	0.04
N	0.04	0.04	0.04
Mg	–	–	0.5
Ti	–	–	0.1
Ni	–	–	0.2
Mn	–	–	0.4
Zn	–	–	0.2

Before being introduced into the technological process, all oxide powder components were dried to remove adsorbed moisture in a SNOL-type drying oven (t = = 90 °C, τ = 1 h). After dosing the components to achieve the target alloy composition, the reagents were mixed in an MP4/5.0 planetary ball mill with a drum volume of up to 5 L for 15—20 min, with a ball-to-powder mass ratio of 1:10.

To prepare the reaction mold, a pre-dried (for at least 1 h at 90 °C) refractory mold made of electrolytic corundum (Al_2O_3) produced by NTC Bakor (Shcherbinka, Moscow Region) was used. The mold was placed on a vibration table, where the mixture was loaded and compacted. Depending on the mold volume, the batch weight during different stages of the experiments ranged from 0.5 to 2.6 kg.

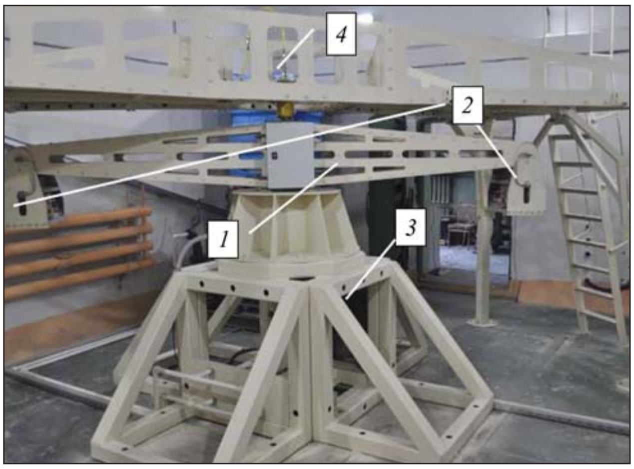

Fig. 1. External view of the centrifugal setup for producing cast materials using centrifugal SHS casting

1 – rotor of the centrifugal setup, ***2*** – reaction chamber, ***3*** – electric drive, ***4*** – laser initiation system

Рис. 1. Внешний вид центробежной установки для получения литых материалов методом центробежного СВС-литья

1 – ротор центробежной установки, ***2*** – реакционный блок, ***3*** – электропривод, ***4*** – система подачи лазерного инициирования

The prepared mold containing the mixture was installed on the rotor of the centrifugal SHS setup, an external view of which is shown in Fig. 1. The design of the SHS setup is proprietary [6; 7; 13] and includes the following systems: laser initiation; automatic rotor speed control to maintain the specified overload level (g); water cooling of the reaction (melting) chamber; and video monitoring with real-time recording of the combustion process.

The synthesis of the target alloy was carried out in an open-type reaction mold at atmospheric pressure and a steady rotor speed corresponding to an overload of $55 \pm 5g$. The combustion temperature exceeded 3000 K, which was higher than the melting point of the final products. After the combustion process was completed, phase separation and crystallization of the reaction products took place under the action of centrifugal forces and due to the mutual immiscibility of the phases. Cooling of the reaction mass was carried out by forced cooling through a water-cooled jacket of the reaction chamber. The combustion products formed an ingot consisting of two distinct layers with a clearly defined interface: the upper (slag) layer composed of corundum, and the lower layer containing the target alloy.

Analysis of the alloys. The quantitative analysis of major elements and impurities was performed using an iCAP 6300 inductively coupled plasma atomic emission spectrometer (Thermo Fisher Scientific, USA), equipped with a double-focusing Nier—Johnson geometry mass analyzer. Carbon and sulfur contents were measured using an SC844 analyzer (LECO, USA), while oxygen, nitrogen, and hydrogen contents were determined using an ONH836 analyzer (LECO, USA).

The phase composition was analyzed by *X*-ray diffraction (XRD) using a DRON 3M diffractometer (ARL X'TRA, Switzerland). Microstructural studies were carried out using a Zeiss Ultra Plus Field Emission Scanning Electron Microscope (Ultra 55 platform, Zeiss, Germany).

Thermodynamic analysis. To estimate the maximum achievable adiabatic synthesis temperature for different initial component ratios, a preliminary thermodynamic analysis was performed using the Thermo software package. Functional additives were excluded from the thermodynamic calculations due to their low concentrations. The calculations provided the equilibrium composition of both condensed and gaseous products, along with the adiabatic reaction temperature.

Results and discussion

The thermodynamic calculation results obtained using the Thermo software package are shown in Fig. 2—4.

Analysis of the obtained data, including adiabatic temperature and component concentrations under conditions of thermodynamic equilibrium, showed that in the Mo—Cr system, the combustion temperature of the exothermic mixture can reach up to 3500 °C. It should be noted that in the molybdenum concentration range of 50—65 wt. %, the temperature ranges from 2800 to 3200 °C, which exceeds the melting points of the components. These conditions are sufficient for obtaining cast materials during the combustion of the investigated mixtures, with the concentration of gaseous products remaining relatively low (less than 0.1 wt. %).

Analysis of the data for the W—Cr system revealed a similar qualitative trend. In the tungsten concentration range of 40—60 wt. %, the combustion temperature exceeds 3000 °C, which ensures complete dissolution of W in molten Cr. At the same time, the content of gaseous products is negligible (less than 0.05 wt. %).

Based on these results, it can be concluded that for the production of cast materials in the studied Mo—Cr and W—Cr systems, at molybdenum oxide (αMoO_3) and tungsten oxide (αWO_3) concentrations exceeding $\alpha = 0.3$, there are no thermodynamic barriers to synthesis. In other words, the calculated combustion temperatures are sufficient to produce cast materials with the target compositions.

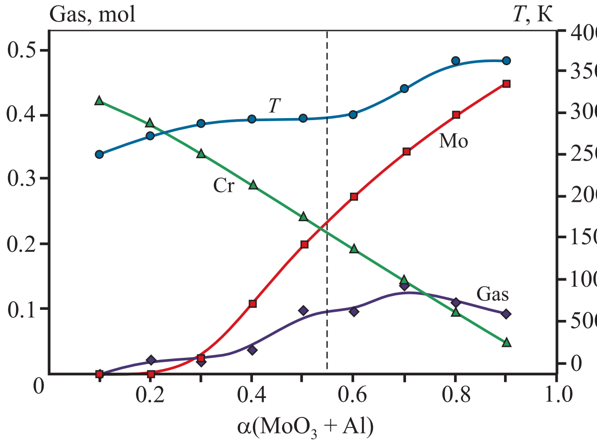

Fig. 2. Results of thermodynamic analysis for the Cr–Mo system at varying composition ratios $(1 - \alpha)(Cr_2O_3 + Al) + \alpha(MoO_3 + Al)$

Рис. 2. Результаты термодинамического анализа системы Cr–Mo при варьировании соотношения составов $(1 - \alpha)(Cr_2O_3 + Al) + \alpha(MoO_3 + Al)$

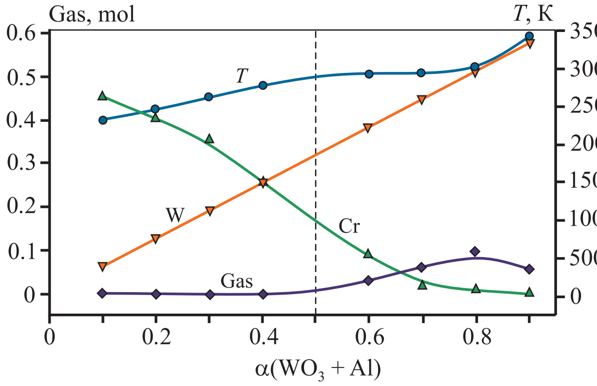

Fig. 3. Results of thermodynamic analysis for the Cr–Mo system at varying composition ratios $(1 - \alpha)(Cr_2O_3 + Al) + \alpha(WO_3 + Al)$

Рис. 3. Результаты термодинамического анализа системы Cr–W при варьировании соотношения составов $(1 - \alpha)(Cr_2O_3 + Al) + \alpha(WO_3 + Al)$

The thermodynamic analysis of the Al—Cr system was carried out considering the use of either chromium (VI) oxide (Fig. 4, *a*) or chromium (III) oxide (Fig. 4, *b*) as the initial component. The results showed that within the target concentration range of 10—25 wt. % Al in the master alloy, the adiabatic combustion temperature reaches approximately 2300 °C for the Cr_2O_3—Al system and around 3000 °C for the CrO_3—Al system. Based on these results, and considering the melting point of chromium, it was decided to use a combined chromium oxide mixture $[Cr_2O_3 + CrO_3]$ in a 50/50 ratio during synthesis.

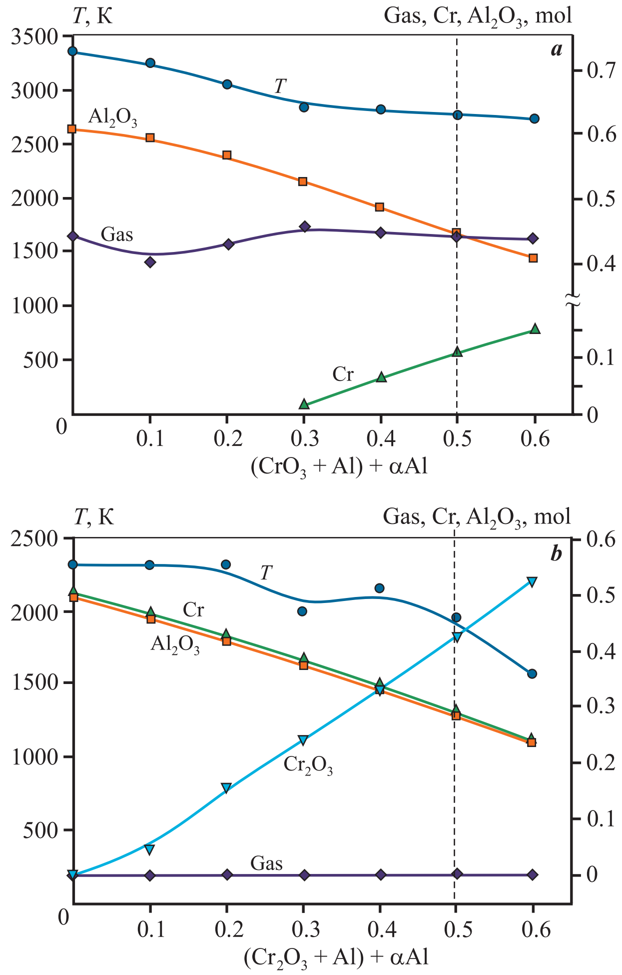

Fig. 4. Results of thermodynamic analysis for the Al–Cr system performed in the "Thermo" software package, considering the use of CrO_3 (***a***) and Cr_2O_3 (***b***)

Рис. 4. Результаты термодинамического анализа системы Al–Cr в программном пакете «Thermo» с учетом применения CrO_3 (***a***) и Cr_2O_3 (***b***)

This approach was justified by the resulting increase in adiabatic temperature to approximately 2500—2700 °C, as well as the formation of pure chromium (complete reduction of chromium oxide) in the reaction products.

When developing the charge compositions and selecting process parameters to obtain alloys with the target compositions, it is essential to have general data on the interaction characteristics of the studied materials as a function of temperature under equilibrium conditions. Such data can be extracted from the analysis of phase diagrams. The phase diagrams used in this study are provided in sources [19—24].

Analysis of the Mo—Cr system [19; 20; 22] showed that both components exhibit unlimited mutual solubility, which will naturally contribute to a more uniform distribution of components within the ingot during synthesis.

A similar interaction pattern was found for the W—Cr system [23], where both components also have unlimited mutual solubility. It should be noted that within the specified component ratio range, the melting point is approximately 2100 °C.

Analysis of the Al—Cr system [24] showed that the general interaction characteristics of the main components favor the formation of various phases (AlCr, $AlCr_2$, αAl_8Cr_5, βAl_8Cr_5, etc.) during cooling and crystallization. It is important to emphasize that within the specified composition range, the melting point is ~1650÷1700 °C.

Effect of FAs on phase separation efficiency

The effect of functional additives on the formation of the sample's macrostructure and the efficiency of phase separation was evaluated using the Cr—Mo alloy system as an example. Two compounds were introduced into the mixture as functional additives: fluorite CaF_2 (fluorspar) and sodium hexafluoroaluminate $Na_3[AlF_6]$ (cryolite). The primary role of these additives is to lower the melting point of the slag phase and, consequently, to reduce its viscosity. This creates favorable conditions for more complete phase separation between the metallic (target) phase and the oxide (slag) phase, ensuring the formation of a clearer phase boundary.

Fig. 5 shows the external appearance of a Cr—Mo alloy sample produced without the use of functional additives in the initial composition. It can be seen that the phase separation process was incomplete, as no distinct phase boundary is observed across the entire cross-section of the ingot. This results in reduced recovery of the target product and significantly complicates phase separation after crystallization and cooling. The loss of the target alloy can reach up to 25 wt. %, which is unacceptable. According to the literature [25; 26], the introduction of calcium oxide (CaO) into an aluminum oxide melt leads to a reduction in melting temperature. Analysis of the CaO—Al_2O_3 phase diagram indicates that even a minor CaO addition (less than 10 %) reduces the melting temperature by approximately 150 °C.

Both the combined FA and a specified amount of calcium fluoride (CaF_2) mixture were used in the experiments. This made it possible to lower the melting temperature of the slag phase by 100—120 °C and to solve two additional problems. At temperatures above its melting point (CaF_2 melts at 1360 °C), this compound decomposes into Ca and F. Each of these elements plays a distinct role when entering the high-temperature melt of combustion products. Fluorine, being highly reactive, interacts with harmful impurities, helping to remove

Fig. 5. Cr–Mo alloy sample produced without functional additives

a – external view of the sample (cross-sectional fracture) after combustion of the mixture); ***b*** – ceramic mold

Рис. 5. Полученный образец системы Cr–Mo без использования функциональной добавки

a – внешний вид образца (поперечный скол) после сжигания смеси; ***b*** – керамическая форма

Fig. 6. External view of the macrostructure of ingots (mass 1–1.45 kg) synthesized for the Cr–Mo (Al) (***a***), Cr–W (Al) (***b***), and Cr–Al (***c***) alloys

Рис. 6. Внешний вид макроструктуры слитков (массой 1–1,45 кг) синтезированных сплавов Cr–Mo (Al) (***a***), Cr–W (Al) (***b***) и Cr–Al (***c***)

them. In particular, fluorine reacts with sulfur according to the reaction $S + 3F_2 \rightarrow SF_6$ forming a colorless, odorless gas. The beneficial effect of elemental calcium is twofold. In the initial stage, calcium acts as a getter in the melt and actively participates in the deoxidation reaction ($Ca + O \rightarrow CaO$) of the melt by reacting with residual (dissolved) oxygen in the alloy, thereby reducing its concentration. In the second stage, calcium oxide (CaO), acting as part of the slag phase, floats to the surface and interacts with molten aluminum oxide, reducing the melting point of the slag phase. This increases the time the melt remains in the liquid state, thus improving the efficiency of phase separation between the metallic and oxide layers.

The phase diagram of the Na_3AlF_6—Al_2O_3 system is relatively simple, with a low eutectic temperature of 961 °C, which further promotes more complete phase separation of the reaction products.

Therefore, the introduction of FAs positively influences phase separation, ensuring a sharply defined boundary, which simplifies the separation of phases after minimal mechanical impact (e.g., tapping).

The optimized concentrations of the mixture components and FA (total content in the initial mixture) are not disclosed, as they constitute proprietary know-how.

All subsequent synthesis experiments for the studied alloys were performed with FA added. The external appearance of the ingot macrostructures obtained for each of the studied alloy systems is shown in Fig. 6.

Cr–Mo (Al) system

The synthesis reaction for this alloy was calculated to achieve the target composition of Cr40Mo56Al4 (wt. %). It is worth noting that the calculated concentrations of the main components for the studied alloys fit well within the permissible ranges specified in Table 2.

As established during the preliminary stage of the study, the ingots produced in the Cr–Mo (Al) alloy initially showed a slight (1–2 %) deficiency in molybdenum content, indicating incomplete reduction. Consi-

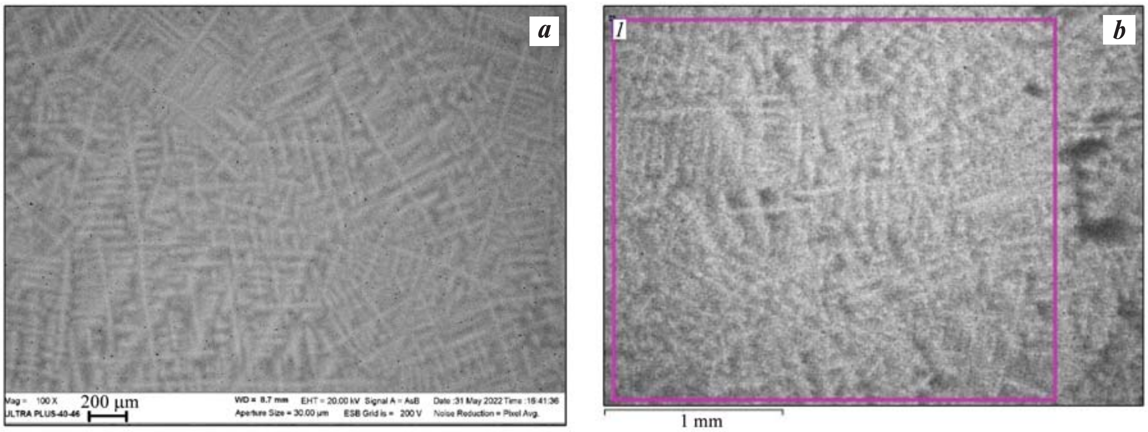

c

Spectrum	Content, wt. %			
	Al	Cr	Mo	Σ
1	3.38	38.00	58.62	100.00

Fig. 7. Microstructure (***a***, ***b***) and EDS composition analysis (***b***, ***c***) of the Cr–Mo (Al) alloy sample (from a polished cross-section)

Рис. 7. Микроструктура (***a***, ***b***) и микроанализ (EDS) состава (***b***, ***c***) полученного образца сплава на основе системы Cr–Mo (Al) (со шлифа)

dering this, a minor adjustment was made in the following experiments, slightly increasing the proportion of molybdenum oxide in the initial mixture compared to the calculated composition.

Fig. 7 presents micrographs of the synthesized cast Cr—Mo (Al) alloy produced under optimized conditions (55*g*, batch weight 1.7 kg, with functional additives). Structural analysis of the obtained material showed a dendritic structure (Fig. 7, *a*), which is characteristic of cast alloys. According to EDS microanalysis performed on a polished cross-section (Fig. 7, *b*), the alloy composition closely matches the calculated target composition (Fig. 7, *c*) in terms of the concentrations of the key elements (see Table 2). This confirms that the selected ratios of the initial components in the mixture were appropriate. Microanalysis of the composition at different locations (top, bottom, and center) of the Cr—Mo (Al) alloy ingot revealed no significant variation in elemental composition across the ingot.

X-ray phase analysis of the synthesized alloy detected only peaks corresponding to the target alloy (a solid solution of Cr in Mo), as shown in Fig. 8. The main XRD parameters for the obtained Cr—Mo (Al) master alloy were: anode — Cu, start angle — 20°, end angle — 100°, step size = 0.02°, scan speed — 0.5 °/s, maximum count — 2063.

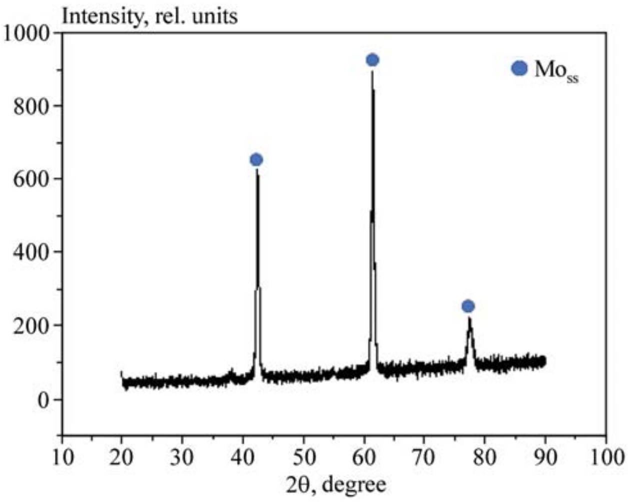

Fig. 8. *X*-ray diffraction analysis of the Cr–Mo (Al) alloy ingot
Mo_{ss} – Mo-based solid solution

Рис. 8. Рентгенофазовый анализ полученного слитка системы Cr–Mo (Al)
Mo_{ss} – твердый раствор на основе Mo

The obtained data indicate that no interaction products were formed between the ceramic mold material and the high-temperature melt of the synthesis products, despite the elevated melt temperature. The resulting alloy composition falls within the permissible concentration range specified for the studied alloys (see Table 2).

Cr—W (Al) system

Due to the higher melting point of tungsten, it was decided to slightly reduce the concentration of this refractory component compared to the base composition

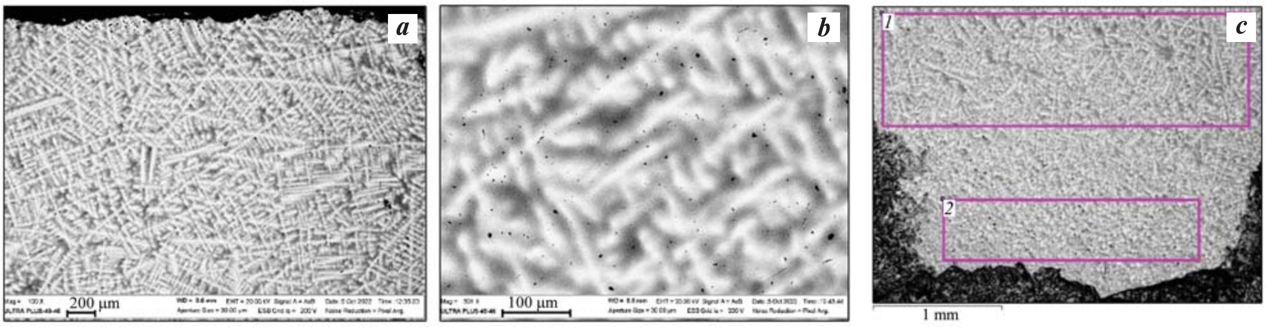

d

Spectrum	Content, wt. %			
	Al	Cr	W	Σ
1	2.91	46.73	50.36	100.00
2	3.85	46.13	50.02	100.00

Fig. 9. Microstructure (***a***, ***b***) and EDS composition analysis (***c***, ***d***) of the Cr–W (Al) alloy sample (from a polished cross-section)

Рис. 9. Микроструктура (***a***, ***b***) и микроанализ (EDS) состава (***c***, ***d***) полученного образца сплава на основе системы Cr–W (Al) (со шлифа)

calculated for the first system (Cr—Mo (Al)). As a result, the Cr43W53Al4 (wt. %) composition was selected as the base composition for the experiments.

Micrographs of the structure and structural components of the synthesized cast Cr—W (Al) alloy samples are shown in Fig. 9, *a*—*c*. Structural analysis confirmed that the obtained alloy also exhibits a well-defined dendritic structure. At higher magnification (Fig. 9, *b*), contrast variations reveal dendritic redistribution of the target alloying elements. The central part of the dendrite arms is enriched in W, while the peripheral region is enriched in Cr. This allowed for detailed point chemical analysis using the INCA Energy 350 XT microanalysis system, installed on the ultra-high-resolution field emission scanning electron microscope. However, this redistribution occurs at the microscale and does not affect the overall quality of the produced alloy.

Microanalysis of the composition at different locations (top, bottom, and center) of the Cr—W (Al) alloy sample showed no significant variations in composition. This is primarily explained by the specific features of SHS metallurgy and the action of centrifugal forces, which promote thorough mixing of the melt components prior to crystallization. The most representative composition data for the obtained alloy are presented in Fig. 9, *c*, *d*. It can be seen that the alloy composition meets the target element concentration requirements (see Table 2), confirming the correct selection of the initial component ratios in the starting mixture.

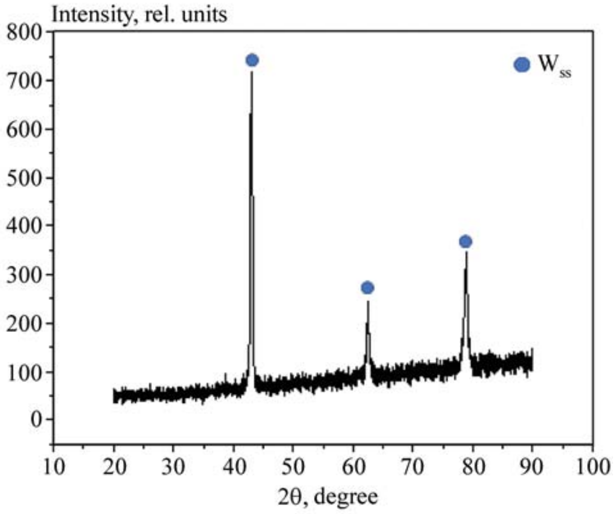

Fig. 10. *X*-ray diffraction analysis of the Cr–W (Al) alloy ingot
W_{ss} – W-based solid solution

Рис. 10. Рентгенофазовый анализ полученного слитка системы Cr–W (Al)
W_{ss} – твердый раствор на основе W

X-ray phase analysis of the synthesized Cr—W (Al) alloy revealed the presence of peaks corresponding to a solid solution formed based on the target elements (a solid solution of Cr in W), as shown in Fig. 10. The main XRD parameters for the Cr—W master alloy were: anode — Cu, start angle — 20°, end angle — 100°, step size — 0.02°, scan speed — 0.5 °/s, maximum count — 1780.

As shown, no unwanted secondary phases were detected in the obtained alloy. Even at this stage of research, it can already be confidently concluded that

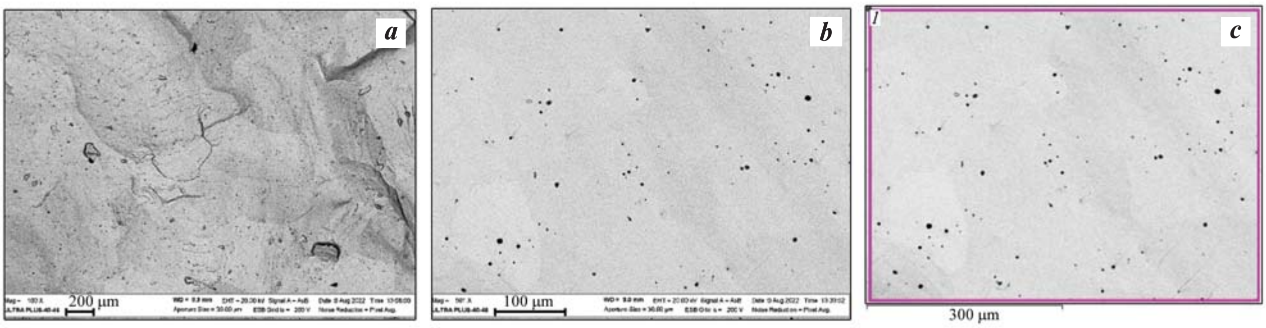

d

Spectrum	Content, wt. %			
	Cr	Al	O	Σ
1	87.71	11.42	0.87	100.00

Fig. 11. Microstructure (***a***, ***b***) and EDS composition analysis (***c***, ***d***) of the Cr–Al alloy sample (from a polished cross-section)

Рис. 11. Микроструктура (***a***, ***b***) и микроанализ (EDS) состава (***c***, ***d***) полученного образца сплава на основе системы Cr–Al (со шлифа)

the use of alundum molds is justified for producing the studied alloys via centrifugal SHS metallurgy.

Cr–Al system

Micrographs of the synthesized cast Cr–Al alloy sample at different magnifications are shown in Fig. 11, *a*, *b*. At higher magnification (Fig. 11, *b*), non-metallic inclusions (slag phase) can be seen in the ingot, which is an expected result at this stage of research (preliminary series of experiments). This is because the reactive mixture mass for this system was insufficient, not exceeding 550 g. During combustion, due to intense heat transfer, the sample cools rapidly, resulting in incomplete phase separation of the synthesis products. This issue is typically resolved by increasing the reactive mixture mass, which is planned for future experiments.

EDS microanalysis performed on the fracture surface (Fig. 11, *c*, *d*) confirms that the alloy composition meets the target element concentration requirements (see Table 2). The residual oxygen content indicates the presence of non-metallic inclusions, resulting from the short "lifetime" of the liquid phase (melt). This limited time prevented the complete reduction of the chromium oxide and did not allow the formed Al_2O_3 to fully transition into the slag phase.

X-ray phase analysis of the synthesized Cr–Al alloy detected only peaks corresponding to the target alloy formed from the main elements (Fig. 12). The main XRD parameters for the Cr–Al master alloy were: anode — Cu, start angle — 20°, end angle — 100°, step size — 0.02°, scan speed — 0.5 °/s, maximum count — 1570.

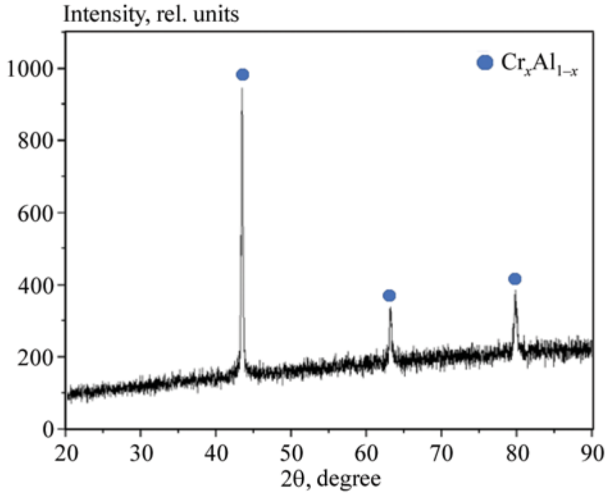

Fig. 12. *X*-ray diffraction analysis of the Cr–Al alloy ingot

Рис. 12. Рентгенофазовый анализ полученного слитка системы Cr–Al

Chemical analysis of the synthesized alloys

When developing chemical methods for alloy production, such as SHS metallurgy, the composition of the reaction mixture is one of the most critical parameters. This composition determines key process conditions, including temperature, reduction efficiency (completeness of reduction of the initial components), and the separation of the slag and metallic phases. In addition to ensuring that the alloy meets the target chemical composition in terms of the main elements, it is also important to monitor the presence and concentrations of impurities. Comprehensive composition control, including all trace elements, is essential for achieving stable and reproducible physical and mechanical properties in advanced high-strength metallic materials.

Tables 3—5 present the full chemical analysis of the synthesized alloys, performed using inductively coupled plasma mass spectrometry (ICP-MS). This method combines an inductively coupled plasma ion source with a mass spectrometer for ion separation and detection and is considered one of the most advanced techniques in modern materials analysis.

In modern metallurgical production, considerable attention is given to the mass fraction of various gases present in metals. The key gases that influence alloy properties are nitrogen, oxygen, and hydrogen. The most commonly used method for determining gas content in metals is combustion analysis, which enables the detection of gas impurities with an accuracy of up to 0.00001 %. Table 6 presents the results of the analysis of the synthesized Cr—Mo and Cr—W alloys for carbon, sulfur, and gas impurities.

Table 3. **Chemical composition of the synthesized Cr—Mo (Al) alloy**

Таблица 3. Результаты химического анализа синтезированного сплава системы Cr–Mo (Al)

Element	Mass fraction, wt. %	Element	Mass fraction, wt. %	Element	Mass fraction, wt. %
Li	<0.0005	Zn	<0.0005	Sm	<0.0003
Be	<0.0003	As	<0.0005	Eu	<0.0003
B	<0.0002	V	<0.0003	Gd	<0.0004
Al	4.27	Rb	<0.0005	Tb	<0.0003
Na	0.0018	Sr	<0.0002	Dy	<0.0007
Mg	<0.0003	Y	<0.0002	Ho	<0.0003
Si	0.4271	Ga	<0.0007	Er	<0.0003
Ca	<0.0003	Ge	<0.0008	Tm	<0.0001
P	0.0010	Zr	0.0005	Yb	<0.0002
K	0.0020	Nb	<0.001	Lu	<0.0005
Sc	<0.0003	Mo	53.02	Hf	<0.0001
Ti	0.0025	Sn	<0.001	Pt-e	<0.002
Cr	42.51	Sb	<0.0003	Re	<0.0002
Fe	0.2110	Ba	<0.0001	W	0.0564
Mn	<0.0002	La	<0.0003	Pb	<0.0003
Co	<0.0005	Ce	<0.0006	Th	<0.0002
Ni	0.0043	Pr	<0.0005	U	<0.0005
Cu	<0.001	Nd	<0.0007	Ta	0.0011

Table 4. **Chemical composition of the synthesized Cr—W (Al) alloy**

Таблица 4. Результаты химического анализа синтезированного сплава системы Cr–W (Al)

Element	Mass fraction, wt. %	Element	Mass fraction, wt. %	Element	Mass fraction, wt. %
Li	<0.0005	Zn	0.0010	Sm	<0.0003
Be	<0.0003	As	<0.0005	Eu	<0.0003
B	<0.0002	V	<0.0003	Gd	<0.0004
Al	4.82	Rb	<0.0005	Tb	<0.0003
Na	0.0019	Sr	0.0006	Dy	<0.0007
Mg	<0.0003	Y	<0.0002	Ho	<0.0003
Si	0.4509	Ga	<0.0007	Er	<0.0003
Ca	<0.0003	Ge	<0.0008	Tm	<0.0001
P	0.0011	Zr	0.0020	Yb	<0.0002
K	0.0062	Nb	<0.001	Lu	<0.0005
Sc	<0.0003	Mo	<0.0006	Hf	<0.0001
Ti	0.0218	Sn	<0.001	Pt-e	<0.002
Cr	42.17	Sb	<0.0003	Re	<0.0002
Fe	0.2131	Ba	<0.0001	W	52.61
Mn	0.0036	La	<0.0003	Pb	0.0019
Co	<0.0005	Ce	<0.0006	Th	<0.0002
Ni	0.0061	Pr	<0.0005	U	<0.0005
Cu	<0.001	Nd	<0.0007	Ta	<0.0005

Table 5. **Chemical composition of the synthesized Cr—Al alloy**

Таблица 5. Результаты химического анализа синтезированного сплава системы Cr–Al

Element	Mass fraction, wt. %	Element	Mass fraction, wt. %	Element	Mass fraction, wt. %
C	0.015	Ni	0.02	Pb	<0.0005
Si	0.15	W	0.06	Sn	<0.001
S	0.002	Fe	0.17	As	0.0006
P	0.012	N	0.0076	Sb	0.001
Cr	85.2	O	0.0017	Bi	<0.0001
Al	12.43	H	0.0021	Zn	0.002
Mo	0.02	Cu	<0.001	Cd	<0.0001

Table 6. **Results of chemical analysis of the synthesized Cr–Mo (Al) and Cr–W (Al) alloys for carbon, sulfur, and gas impurities**

Таблица 6. Результаты химического анализа синтезированных сплавов Cr–Mo (Al) и Cr–W (Al) на наличие углерода, серы и газовых примесей

Alloy	Mass fraction, wt. %				
	C	S	O	N	H
Cr–Mo (Al)	0,011	0,0028	0,042	0,019	0,0014
Cr–W (Al)	0,0091	0,00078	0,12	0,0072	0,0012

Analysis of the obtained chemical composition data allows us to conclude that the synthesized alloys meet all key requirements for permissible concentrations of both target elements and impurities. It is particularly worth noting the low content of harmful impurities such as sulfur and hydrogen.

Conclusion

This study included thermodynamic analyses of combustion temperatures for the investigated exothermic systems Mo—Cr, W—Cr, Cr_2O_3—Al, and CrO_3—Al. These analyses confirmed that there are no thermodynamic barriers to the synthesis of the target materials using SHS metallurgy.

The main conclusions drawn from this work are as follow:

1. A comprehensive series of experiments demonstrated that in the production of master alloys based on refractory elements (Mo—Cr and W—Cr), as well as systems with a significant difference in melting points (Cr—Al), the mass of the reaction mixture should be increased to 1.5—2.0 kg in order to extend the time the melt remains in the liquid state (the melt “lifetime”).

2. The centrifugal acceleration applied should be at least 50 *g*.

3. To increase the synthesis temperature when producing ingots in the Cr—Al system, a combined oxidizer should be used, consisting of a mixture of chromium (III) oxide and chromium (VI) oxide, with the Cr_2O_3/CrO_3 ratio ranging from 70/30 to 40/60.

4. The experiments confirmed the necessity of introducing functional additives at 3 % of the oxidizer mass. These additives should be a combination of cryolite and fluorite, to lower the melting temperature of the slag phase and thereby improve the phase separation between the metallic and oxide phases.

5. Analysis of the Cr—Mo (Al) and Cr—W (Al) master alloys demonstrated the need to introduce an excess amount of MoO_3 and WO_3, respectively, due to the incomplete reduction of Mo and W from their oxides.

6. Microstructural analysis of the obtained master alloys revealed the presence of a dendritic structure, which is typical for cast alloys.

7. *X*-ray phase analysis results highlighted the importance of using a ceramic mold to ensure uniformity of the material’s phase composition.

8. The chemical composition analysis of the synthesized Mo—Cr (Al), W—Cr (Al), and Cr—Al alloys, performed using ICP-MS, confirmed that the target compositions were achieved and fully met the permissible concentration requirements for both target elements and impurities. Particularly noteworthy is the low content of harmful impurities such as sulfur and hydrogen.

References

1. Goldshtein M.I., Grachev S.V., Veksler Yu.G. Special steels. Moscow: MISIS, 1999. 408 p. (In Russ.).
Гольдштейн М.И., Грачев С.В., Векслер Ю.Г. Специальные стали. М: МИСИС, 1999. 408 с.
2. Solntsev Yu.P., Pryakhin E.I., Pirainen V.Yu. Special materials in mechanical engineering. Saint Petersburg: Khimizdat, 2004. 640 p. (In Russ.).
Солнцев Ю.П., Пряхин Е.И., Пирайнен В.Ю. Специальные материалы в машиностроении. СПб.: Химиздат, 2004. 640 с.
3. Lyakishev N.P., Gasik M.I. Metallurgy of chromium. Moscow: Eliz, 1999. 581 p. (In Russ.)
Лякишев Н.П., Гасик М.И. Металлургия хрома. М.: Элиз, 1999. 581 с.
4. Yukhvid V.I., Gorshkov V.A., Sanin V.N., Andreev D.E., Vdovin Yu.S. SHS metallurgy of refractory materials based on molybdenum. In: *Explosive production of new materials: science, technology, business, and innovations:* 14th International Symposium (Saint Petersburg, 14—18 May 2018). Ed. M.I. Alymov, O.A. Golosova. Moscow: Torus Press, 2018. P. 294—297.
5. Structural chromium alloys. Ed. V.I. Trefilov. Kyiv: Naukova Dumka, 1986. 216 p. (In Russ.).
Конструкционные сплавы хрома: Сб. науч. трудов. Отв. ред. В.И. Трефилов. Киев: Наукова думка, 1986. 216 с.
6. Kolobov Yu.R., Manokhin S.S., Kudymova Yu.E., Klimenko D.N., Sanin V.N., Ikornikov D.M., Andreev D.E. SHS-produced cast Ni—Cr—W alloy: structural characterization and mechanical properties. In: *Book of abstracts of XIV International Symposium on Self-Propagating High Temperature Synthesis (SHS-2017)* (Tbilisi, Georgia, 25—28 September 2017). 2017. P. 230—231.

7. Yukhvid V.I., Andreev D.E., Sanin V.N., Sachkova N.V. SHS metallurgy of composite materials based on the Nb—Si system. *Russian Journal of Non-Ferrous Metals.* 2018;59(1):42—49.
8. Ziatdinov M.Kh., Shatokhin I.M., Leont'ev L.I. SHS technology of composition ferroalloys Part I. Metallurgical SHS process. Synthesis of ferrovanadium and ferrochromium nitrides. *Izvestiya. Ferrous Metallurgy.* 2018;61(5):339—347. (In Russ.).
https://doi.org/10.17073/0368-0797-2018-5-339-347
Зиатдинов М.Х., Шатохин И.М., Леонтьев Л.И. Технология СВС композиционных ферросплавов. Часть I. Металлургический СВС процесс. Синтез нитридов феррованадия и феррохрома. *Известия вузов. Черная металлургия.* 2018;61(5):339—347.
https://doi.org/10.17073/0368-0797-2018-5-339-347
9. Ziatdinov M.Kh., Shatokhin I.M., Leont'ev L.I. SHS technology of composition ferroalloys Part II. Synthesis of ferrosilicon nitride and ferrotitanium boride. *Izvestiya. Ferrous Metallurgy.* 2018;61(7):527—535. (In Russ.). https://doi.org/10.17073/0368-0797-2018-7-527-535
Зиатдинов М.Х., Шатохин И.М., Леонтьев Л.И. Технология СВС композиционных ферросплавов. Часть II. Синтез нитрида ферросилиция и борида ферротитана. *Известия вузов. Черная металлургия.* 2018;61(7):527—535.
https://doi.org/10.17073/0368-0797-2018-7-527-535
10. Ziatdinov M.Kh. Metallurgical SHS processes as a route to industrial-scale implementation: An autoreview. *Internationsl Journal of Self-Propagating High-Temperature Synthesis.* 2018;27(1):1—13.
https://doi.org/10.3103/S1061386218010132
11. Sanin V.N., Yukhvid V.I., Andreev D.E., Alymov M.I. Centrifugal SHS metallurgy. Solving practical problems. In: *Material-forming highly exothermic processes: metallothermy and combustion of thermite-type systems.* Ed. M.I. Alymov. Moscow: RAS, 2021. Chapter 7. P. 321–372. (In Russ.).
Санин В.Н., Юхвид В.И., Андреев Д.Е., Алымов М.И. Центробежная СВС-металлургия. Решение практических задач. В кн. *Материалообразующие высокоэкзотермические процессы: металлотермия и горение систем термитного типа.* Под общ. ред. М.И. Алымова. М.: РАН, 2021. Глава 7. С. 321—372.
12. Yukhvid V.I., Ikornikov D.M., Andreev D.E., Sanin V.N., Alymov M.I., Sachkova N.V., Semenova V.N., Kovalev I.D. Centrifugal SHS-metallurgy of nitrogen steels. *Letters on Materials.* 2018;8(4(32)):499—503.
13. Yukhvid V.I., Gorshkov V.A., Sanin V.N. Production of new ceramic and composite materials using SHS metallurgy methods. In: *Technological combustion.* Eds. S.M. Aldoshin, M.I. Alymov. Moscow: Institute of Problems of Chemical Physics of the RAS, 2018. Chapter 14. P. 350—371. (In Russ.).
https://doi.org/10.31857/S9785907036383000014
Юхвид В.И., Горшков В.А., Санин В.Н. Получение новых керамических и композиционных материалов методами СВС-металлургии. В кн. *Технологическое горение.* Под общ. ред. С.М. Алдошина, М.И. Алымова. М.: ИПХФ РАН, 2018. Глава 14. С. 350—371.
https://doi.org/10.31857/S9785907036383000014
14. Sanin V., Andreev D., Ikornikov D., Yukhvid V. Cast intermetallic alloys and composites based on them by combined centrifugal casting — SHS process. *Open Journal of Metal.* 2013;3(2B):12—24.
https://doi.org/10.4236/ojmetal.2013.32A2003
15. Lyakishev N.P., Gasik M.I., Dashevsky V.Ya. Metallurgy of ferroalloys. Part 1. Metallurgy of silicon, manganese and chromium alloys. Moscow: MISIS, 2006. 117 p. (In Russ.).
Лякишев Н.П., Гасик М.И., Дашевский В.Я. Металлургия ферросплавов. Ч. 1. Металлургия сплавов кремния, марганци и хрома: Учеб. пос. М.: МИСИС, 2006. 117 с.
16. Yukhvid V.I., Andreev D.E., Sanin V.N., Gorshkov V.A., Alymov M.I. Synthesis of cast composite materials by SHS metallurgy methods. *Key Engineering Materials.* 2017;(746):219—232.
https://doi.org/10.4028/www.scientific.net/KEM.746.219
17. Sanin V.N., Ikornikov D.M., Golosova O.A., Andreev D.E., Yukhvid V.I. Centrifugal SHS metallurgy of cast Co—Cr—Fe—Ni—Mn high-entropy alloys strengthened by precipitates based on Mo and Nb borides and silicides. *Physical Mesomechanics.* 2021;24(6):692—700.
https://doi.org/10.1134/S1029959921060072
18. Sanin V.N., Yukhvid V.I., Andreev D.E., Ikornikov D.M., Levashov E.A., Pogozhev Yu.S. SHS of cast refractory alloys for reprocessing into micro granules used in 3D additive technologies. In: *Book of abstracts of XIV International Symposium on Self-Propagating High Temperature Synthesis (SHS-2017)* (Tbilisi, Georgia, 25—28 September 2017). 2017. P. 224—226.
19. Bannykh O.A., Budberg P.B., Alisova S.P. State diagrams of binary and multicomponent iron-based systems. Moscow: Metallurgiya, 1986. 440 p. (In Russ.).
Банных О.А., Будберг П.Б., Алисова С.П. Диаграммы состояния двойных и многокомпонентных систем на основе железа. М.: Металлургия, 1986. 440 с.
20. Lyakishev N.P. Phase diagrams of binary metal systems. Moscow: Mashinostroenie, 1997. Vol. 2. 1023 p. (In Russ.).

Лякишев Н.П. Диаграммы состояния двойных металлических систем. М.: Машиностроение, 1997. Т. 2. 1023 с.

21. Kocherzhinskii Yu.A., Vasilenko V.I. Fusibility diagrams of the systems Mo—Nb (V, Cr), V—Nb (Cr), and Mo—V—Nb (Cr). *Russian Metallurgy (Metally).* 1985;(2):186—190.
22. Kocherzhinskii Yu.A., Vasilenko V.I. Fusibility diagram of molybdenum—chromium. *Russian Metallurgy (Metally).* 1979;(4):205—207.
23. Nagender Naidu S.V., Sriramamurthy A.M., Rama Rao P. The Cr—W (chromium—tungsten) system. *Bulletin of Alloy Phase Diagrams.* 1984;5(3):289—307.
24. Alisova S.P., Budberg P.B., Ageev N.V. Phase diagrams of metallic systems. Moscow: VINITI, 1975. 268 p. (In Russ).
    Алисова С.П., Будберг П.Б., Агеев Н.В. Диаграммы состояния металлических систем. М.: ВИНИТИ, 1975. 268 с.
25. Nurse R.W., Welch J.H., Majumdar A.J. The CaO—Al_2O_3 system in a moisture-free atmosphere. *Transactions of the British Ceramic Society.* 1965;64:409—418.
26. Nurse R.W., Welch J.H., Majumdar A.J. The 12CaO·7Al_2O_3 phase in the CaO—Al_2O_3 system. *Transactions of the British Ceramic Society.* 1965;64:323—382.

Information about the authors

Anastasiya N. Kubanova – Graduate Student of the Merzhanov Institute of Structural Macrokinetics and Materials Science of the Russian Academy of Sciences (ISMAN), Junior Research Scientist of Tula State Pedagogical University n.a. L.N. Tolstoy.
https://orcid.org/0000-0001-6685-1447
E-mail: kubanovaan@tsput.ru

Denis M. Ikornikov – Research Scientist, ISMAN.
https://orcid.org/0000-0002-8082-4442
E-mail: denis-ikornikov@yndex.ru

Vladimir N. Sanin – Dr. Sci. (Eng.), Senior Research Scientist, ISMAN.
https://orcid.org/0000-0001-8402-4605
E-mail: svn@ism.ac.ru

Dmitry A. Martynov – General Manager of LLC "Research, Design and Technology Center".
E-mail: martynov@rdtcenter.com

Информация об авторах

Анастасия Николаевна Кубанова – аспирант Института структурной макрокинетики и проблем материаловедения им. А.Г. Мержанова РАН (ИСМАН), мл. науч. сотрудник Тульского государственного педагогического университета им. Л.Н. Толстого.
https://orcid.org/0000-0001-6685-1447
E-mail: kubanovaan@tsput.ru

Денис Михайлович Икорников – науч. сотрудник ИСМАН.
https://orcid.org/0000-0002-8082-4442
E-mail: denis-ikornikov@yndex.ru

Владимир Николаевич Санин – д.т.н., ст. науч. сотрудник ИСМАН.
https://orcid.org/0000-0001-8402-4605
E-mail: svn@ism.ac.ru

Дмитрий Александрович Мартынов – ген. директор ООО «Центр исследований, дизайна и технологий».
E-mail: martynov@rdtcenter.com

Contribution of the authors

A.N. Kubanova – literature review, analysis of experimental data, manuscript writing.

D.M. Ikornikov – preparation of mixtures and raw materials, experimental work, participation in result discussions.

V.N. Sanin – definition of the research objective, experimental work, participation in result discussions, manuscript editing.

D.A. Martynov – problem formulation and definition of the research objective, participation in result discussions.

Вклад авторов

А.Н. Кубанова – анализ литературных данных, работа с экспериментальными данными, написание статьи.

Д.М. Икорников – подготовка материалов для экспериментов, проведение экспериментов, участие в обсуждении результатов.

В.Н. Санин – определение цели работы, проведение экспериментов, участие в обсуждении результатов, редактирование статьи.

Д.А. Мартынов – описание проблемы и определение цели работы, участие в обсуждении результатов.

The article was submitted 08.04.2024, revised 18.07.2024, accepted for publication 22.07.2024

Статья поступила в редакцию 08.04.2024, доработана 18.07.2024, подписана в печать 22.07.2024